www.elsevier.nl/locate/jorganchem

Journal of Organometallic Chemistry 607 (2000) 27–40

Syntheses and structural studies of five- and six-coordinate *o*-halophenyl derivatives of ruthenium(II) and osmium(II)

Clifton E.F. Rickard, Warren R. Roper* [1], Scott D. Woodgate, L. James Wright* [2]

Department of Chemistry, The University of Auckland, Private Bag 92019, Auckland, New Zealand

Received 4 February 2000; received in revised form 3 March 2000

Dedicated to Professor Martin A. Bennett on the occasion of his retirement from the Research School of Chemistry, The Australian National University.

Abstract

Reaction between $MHCl(CO)(PPh_3)_3$ (M = Ru, Os) and the *o*-halophenyl mercury compounds, $Hg(C_6H_4X\text{-}2)_2$ (X = Cl, Br, I) gives the five co-ordinate complexes, $M(C_6H_4X\text{-}2)Cl(CO)(PPh_3)_2$ (**1a** M = Ru, X = Cl; **1b** M = Ru, X = Br; **2a** M = Os, X = Cl; **2b** M = Os, X = Br; **2c** M = Os, X = I). In these complexes there is a significant bonding interaction between the coordinatively unsaturated metal centre and the *o*-halo-substituent on the σ-bound phenyl group as revealed by crystal structure determinations of **2a**, **2b**, and **2c**. Each of the five-coordinate complexes readily adds CO forming the corresponding six-coordinate dicarbonyl complexes, $M(C_6H_4X\text{-}2)Cl(CO)_2(PPh_3)_2$ (**5a** M = Ru, X = Cl; **5b** M = Ru, X = Br; **6a** M = Os, X = Cl; **6b** M = Os, X = Br; **6c** M = Os, X = I). Crystal structure determination of **6a** confirms regular octahedral geometry for these six-coordinate complexes with no interaction between the metal centre and the *o*-halo-substituent on the σ-bound phenyl group. The complexes **1a**, **b**, **2a**–**c**, **5a**, **b**, **6a**–**c**, are potentially precursors of benzyne complexes through reduction (removal of ClX) but all attempts at reduction were unsuccessful. The related thiocarbonyl complexes, $Os(C_6H_4X\text{-}2)Cl(CS)(PPh_3)_2$ (**7a** X = Cl; **7b** X = Br) and $Os(C_6H_4X\text{-}2)Cl(CO)(CS)(PPh_3)_2$ (**8a** X = Cl; **8b** X = Br), have been prepared similarly beginning with $OsHCl(CS)(PPh_3)_3$. The crystal structure of **8a** has been determined. Both **8a** and **8b** undergo a slow migratory-insertion reaction upon heating to yield the corresponding η^2-thioacyl complexes, $Os(\eta^2\text{-}C[S]C_6H_4X\text{-}2)Cl(CO)(PPh_3)_2$ (**9a** X = Cl; **9b** X = Br), the crystal structures of both of which have been determined. Once the *o*-halophenyl group is no longer directly bonded to the metal, as in **9a** and **9b**, normal reactivity returns to the *o*-halo substituent and **9b** undergoes lithium–bromine exchange when treated with *n*-butyllithium and the resulting lithiated material, when treated with Sn^nBu_3Cl, gives $Os(\eta^2\text{-}C[S]C_6H_4Sn^nBu_3\text{-}2)Cl(CO)(PPh_3)_2$ (**10**). © 2000 Elsevier Science S.A. All rights reserved.

Keywords: Ruthenium; Organometallic complexes; Osmium

1. Introduction

Many examples of *o*-halophenyl derivatives of both main group elements [1] and transition metals [2] (see Fig. 1) are known. One of the main reasons for continuing interest in this class of compounds is that the transition metal derivatives are potential precursors of transition metal benzyne complexes as has been demonstrated by the work of the dedicatee of this paper, Professor M.A. Bennett and his coworkers [3]. We have established that a convenient route to coordinatively unsaturated σ-aryl derivatives of ruthenium and osmium, $M(Ar)Cl(CO)(PPh_3)_2$ involves treatment of $MHCl(CO)(PPh_3)_3$ with $HgAr_2$ [4]. This reaction is general and aryl groups bearing various functionalities have been transferred to ruthenium or osmium. Where the

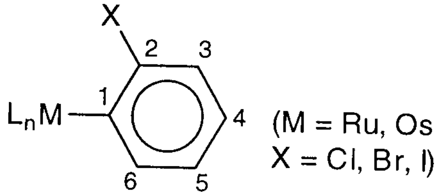

Fig. 1. *o*-Halophenyl complexes of ruthenium(II) and osmium(II).

---

[1] *Corresponding author. Tel.: + 64-9-3737999, ext. 8320; fax: + 64-9-3737422; e-mail: w.roper@auckland.ac.nz

[2] *Corresponding author.

PII: S0022-328X(00)00170-4

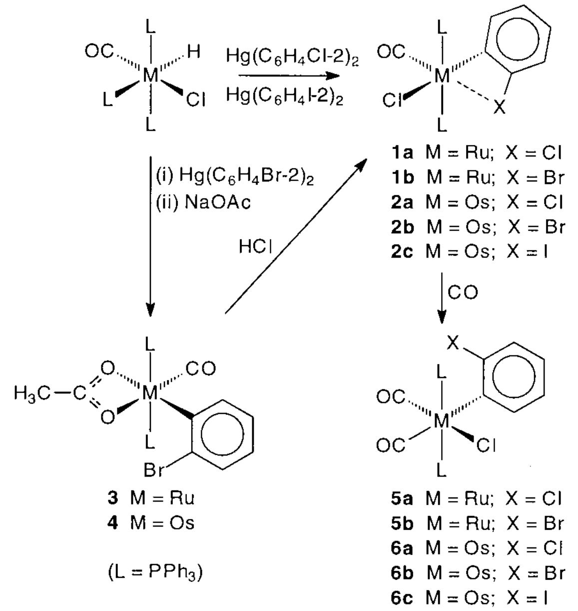

Scheme 1. Synthesis and reactions of the carbonyl-containing *o*-halophenyl complexes, $M(C_6H_4X\text{-}2)Cl(CO)(PPh_3)_2$.

functional group is in the *ortho*-position and contains a potential donor atom there is a chelating interaction with the metal centre, as observed for example in the *o*-nitrophenyl derivatives [5]. The availability of $HgAr_2$ where Ar = *o*-halophenyl [6], presented the possibility of forming the coordinatively unsaturated *o*-halophenyl complexes of ruthenium and osmium. These compounds were of interest both as potential benzyne complex precursors and because of possible interaction of the halo-substituent with the metal centre. In most of the previously reported *o*-halophenyl complexes the metal is coordinatively saturated or has no effective vacant coordination site, e.g. Ni(II), Pt(II), and in these cases there is no structural evidence for a bonding interaction between the *o*-halo substituent and the metal.

In this paper we report (i) the synthesis of a set of five coordinate complexes, $M(C_6H_4X\text{-}2)Cl(CO)(PPh_3)_2$ and the corresponding set of six coordinate complexes, $M(C_6H_4X\text{-}2)Cl(CO)_2(PPh_3)_2$; (ii) comparitive structural studies of examples from both sets which reveal a significant bonding interaction between the halo-substituent and the metal centre in the five coordinate compounds; (iii) the synthesis of thiocarbonyl-containing osmium analogues which undergo migratory insertion reactions forming the corresponding η^2-thioacyl derivatives, $Os(\eta^2\text{-}C[S]C_6H_4X\text{-}2)Cl(CO)(PPh_3)_2$; (iv) investigations of the reduction of these *o*-halophenyl complexes to benzyne complexes; and (v) the lithiation of $Os(\eta^2\text{-}C[S]C_6H_4X\text{-}2)Cl(CO)(PPh_3)_2$ and subsequent stannylation to $Os(\eta^2\text{-}C[S]C_6H_4SnBu^n_3\text{-}2)Cl(CO)(PPh_3)_2$.

2. Results and discussion

2.1. Syntheses of five and six coordinate *o*-halophenyl complexes of ruthenium(II) and osmium(II)

The five coordinate *o*-halophenyl complexes, $M(C_6H_4X\text{-}2)Cl(CO)(PPh_3)_2$ (**1a** M = Ru, X = Cl; **1b** M = Ru, X = Br; **2a** M = Os, X = Cl; **2b** M = Os, X = Br; **2c** M = Os, X = I), were prepared by treatment of $MHCl(CO)(PPh_3)_3$ with $Hg(C_6H_4X\text{-}2)_2$ according to Scheme 1. In the case of X = Br, it proved to be more convenient, not to isolate the five coordinate complex directly, but rather to add sodium acetate and isolate the saturated, η^2-acetato-derivatives, $M(C_6H_4Br\text{-}2)(\eta^2\text{-}O_2CMe)(CO)(PPh_3)_2$ (**3** M = Ru; **4** M = Os). Compounds **3** and **4** are readily converted to **1b** and **2b**, respectively, by treatment with HCl. Addition of CO rapidly converts **1a–b**, **2a–c** to the corresponding colourless, six coordinate, dicarbonyl complexes, **5a–b**, **6a–c**. IR, ^1H- and ^{13}C-NMR data for these and other new compounds reported in this paper are collected in Tables 1–3. As a typical example, the data for **2a** is discussed below. The IR spectrum of complex **2a** shows $\nu(CO)$ at 1912 cm^{-1}, similar to the position observed for $Os(C_6H_4CH_3\text{-}2)Cl(CO)(PPh_3)_2$ [4b]. The ^1H-NMR spectrum reveals signals due to all four of the aromatic ring protons in the region expected. Apparent doublets at 5.60 ($^3J_{HH} = 7.3$ Hz) and 6.14 ppm ($^3J_{HH} = 6.9$ Hz) are assigned to the protons at ring positions 3 and 6 (see Fig. 1 for numbering), respectively. Apparent triplets at 6.19 ($^3J_{HH} = 7.3$ Hz) and 6.41 ppm ($^3J_{HH} = 7.5$ Hz) are assigned to protons at ring positions 4 and 5. The ^{13}C-NMR spectrum shows a triplet for the carbonyl resonance at 179.38 ppm ($^2J_{CP} = 11.0$ Hz), due to coupling to the two identical phosphorus nuclei. The unsubstituted carbons of the chlorophenyl ring are observed as singlets at 121.4, 123.86, 127.93, and 138.43 ppm. The quaternary ring carbons were not observed.

The colour of complexes **1a–b**, **2a–c** are yellow–orange. In contrast, coordinatively unsaturated complexes of the type $M(Ar)Cl(CO)(PPh_3)_2$ which have been prepared previously are usually dark-red in colour [4]. This difference in colour could be indicative of an interaction between the halo-substituent on the aryl ligand, and the metal centre. To examine this possibility, single crystal X-ray structure determinations for **2a–c** were obtained. In addition, the crystal structure of **6a** was obtained to provide information on the structure of a complex where no interaction with the *o*-halo-substituent is possible.

2.2. Crystal structure determinations of **2a–c**, and **6a**

Details of the crystal structure determinations for **2a–c** and **6a**, and for the other crystal structures reported in this paper, are collected in Table 4. Selected bond distances and angles for **2a**–**c** and **6a** are given in Tables 5–8, respectively. Since **2a**–**c** are isostructural, only one ORTEP diagram is shown, that of **2a** in Fig. 2, and the molecular geometry of **6a** is given in Fig. 3.

In all these structures, the two triphenylphosphine ligands are located mutually *trans*. The osmium-bound chloride is *trans* to the C_6H_4X-2 ring with the bond distance, Os–Cl(1) being 2.459(5) Å in **2a**. A conspicuous feature apparent in Fig. 2 is that for the structures of **2a**–**c** the *o*-halophenyl group lies in the plane containing Os, C(1), C(2), and Cl(1), with the *ortho*-halogen substituent making a close approach to osmium. This interaction is accompanied by both a tilting of the ring within the equatorial plane and a reduction of the angle C(2)–C(3)–X from the idealised 120°. These distortions are summarised in Fig. 4 where a comparison is also made with the dicarbonyl analogue **6a**. For **2a** the distance between the *o*-chloro substituent on the phenyl ring and osmium (Os–Cl(2)) is 2.826(4) Å. This is outside the range of previously reported Os–Cl bond distances since a search of the CCD shows that reported Os–Cl distances range from 2.178 to 2.759 Å (560 observations, average 2.380 Å, standard deviation 0.065 Å). Nevertheless, a bonding interaction must be present to account for the significant distortions from idealised geometries that displace the halogen towards the osmium atom. The structural data for **2b** and **2c** show the same distortions involving the *o*-halophenyl group with the distance between the *o*-bromo substituent on the phenyl ring and osmium being 2.8323(8) Å and the corresponding Os–I distance being 2.9335(6) Å. This Os–I distance is only slightly outside the range 2.61–2.87 Å reported in the CCD for osmium–iodide bonds (106 observations, average 2.75 Å, standard deviation 0.095 Å).

Table 1
IR data for *o*-halophenyl ruthenium(II) and osmium(II) complexes

Complex	ν(CO) (cm^{-1})	Other bands (cm^{-1})
$Ru(C_6H_4Cl\text{-}2)Cl(CO)(PPh_3)_2$ (**1a**)	1927, 1916, 1921	1798, 1760, 1601, 1310, 1270
$Ru(C_6H_4Br\text{-}2)Cl(CO)(PPh_3)_2$ (**1b**)	1915	1586, 581
$Os(C_6H_4Cl\text{-}2)Cl(CO)(PPh_3)_2$ (**2a**)	1912	1651, 1572, 1259, 1224
$Os(C_6H_4Br\text{-}2)Cl(CO)(PPh_3)_2$ (**2b**)	1911	1587, 1541, 645
$Os(C_6H_4I\text{-}2)Cl(CO)(PPh_3)_2$ (**2c**)	1902	1710, 1594, 953, 609
$Ru(C_6H_4Br\text{-}2)(\eta^2\text{-}O_2CCH_3)(CO)(PPh_3)_2$ (**3**)	1924	1560, 1526, 753, 743, 668, 595, 543, 510
$Os(C_6H_4Br\text{-}2)(\eta^2\text{-}O_2CCH_3)(CO)(PPh_3)_2$ (**4**)	1914	1564, 1520, 952, 606, 557
$Ru(C_6H_4Cl\text{-}2)Cl(CO)_2(PPh_3)_2$ (**5a**)	2032, 1957	1654, 1400, 800, 668
$Ru(C_6H_4Br\text{-}2)Cl(CO)_2(PPh_3)_2$ (**5b**)	2043, 1961	1608, 1591
$Os(C_6H_4Cl\text{-}2)Cl(CO)_2(PPh_3)_2$ (**6a**)	2018, 1941	1654, 1570, 1405, 668
$Os(C_6H_4Br\text{-}2)Cl(CO)_2(PPh_3)_2$ (**6b**)	2017, 1957, 1940	1587, 1573, 1312, 846, 620, 598
$Os(C_6H_4I\text{-}2)Cl(CO)_2(PPh_3)_2$ (**6c**)	2022, 1939	1716, 1573, 1541, 1313, 847, 663, 597
$Os(C_6H_4Cl\text{-}2)Cl(CS)(PPh_3)_2$ (**7a**)		1654, 1568, 1307 ν(CS), 647
$Os(C_6H_4Br\text{-}2)Cl(CS)(PPh_3)_2$ (**7b**)		1654, 1306 ν(CS)
$Os(C_6H_4Cl\text{-}2)Cl(CS)(CO)(PPh_3)_2$ (**8a**)	2010	1291 ν(CS), 668, 503
$Os(C_6H_4Br\text{-}2)Cl(CS)(CO)(PPh_3)_2$ (**8b**)	2021	1577, 1291, 813, 704, 668, 592
$Os(\eta^2\text{-}C[S]C_6H_4Cl\text{-}2)Cl(CO)(PPh_3)_2$ (**9a**)	1901	1482, 1295, 1236, 668
$Os(\eta^2\text{-}C[S]C_6H_4Br\text{-}2)Cl(CO)(PPh_3)_2$ (**9b**)	1898	1574, 1296, 1263, 810, 635, 618, 592, 577
$Os(\eta^2\text{-}C[S]C_6H_4Sn^nBu_3\text{-}2)Cl(CO)(PPh_3)_2$ (**10**)	1900	1573, 1291, 1261, 824, 596

Instances of haloarenes functioning as ligands towards transition metals are well known. Examples are provided by the structurally characterised *ortho*-diiodobenzene complex of iridium, $[Ir(\eta^2\text{-}I_2C_6H_4)H_2(PPh_3)_2]PF_6$ [7] and the halobenzene complexes of platinum, *trans*-$[Pt(\eta^1\text{-}XPh)H(P^iPr_3)_2]^+$ (X = I, Br) [8].

The dicarbonyl complex, **6a**, has an almost regular octahedral geometry about osmium (see Fig. 3). Introduction of CO saturates the metal centre and a bonding interaction between the *o*-chloro substituent and the osmium is no longer possible. As a consequence, steric effects dominate and the *o*-chlorophenyl ring twists out of the equatorial plane by 28°. Examination of Fig. 4 shows that θ_1 is now greater than 120° whereas for **2a**–**c** the corresponding angle is always considerably less than 120°. The Os–C(3) distance of 2.169(6) Å is longer than the corresponding distances found for compounds **2a**–**c** (see Fig. 4).

2.3. Syntheses of five and six coordinate *o*-halophenyl complexes of osmium(II) incorporating thiocarbonyl ligands

The five coordinate, thiocarbonyl-containing, *o*-halophenyl complexes, $Os(C_6H_4X\text{-}2)Cl(CS)(PPh_3)_2$ (**7a** X = Cl; **7b** X = Br), were prepared by treatment of $OsHCl(CS)(PPh_3)_3$ with $Hg(C_6H_4X\text{-}2)_2$ according to Scheme 2. Both **7a** and **7b** are bright yellow in colour and show strong thiocarbonyl absorptions in the IR spectrum at 1307 cm^{-1} for **7a** and at 1306 cm^{-1} for **7b** (see Tables 1–3 for further spectroscopic data). Addition of CO to **7a** and **7b**, in a rapid reaction, gives the colourless, coordinatively saturated complexes, $Os(C_6H_4X\text{-}2)Cl(CO)(CS)(PPh_3)_2$ (**8a** X = Cl; **8b** X = Br). The crystal structure of **8a** has been determined (see Fig. 5 for molecular geometry and Table 9 for selected bond distances and angles). The structure re-

Table 2
^{1}H-NMR data for *o*-halophenyl ruthenium(II) and osmium(II) complexes

Complex	Chemical shift (ppm)/coupling constant (Hz)
$Ru(C_6H_4Cl\text{-}2)Cl(CO)(PPh_3)_2$ (**1a**)	5.62 (d, 1H, C_6H_4Cl, $^3J_{HH} = 6.8$); 6.15 (t, 1H C_6H_4Cl, $^3J_{HH} = 6.5$); 6.27 (d, 1H, C_6H_4Cl, $^3J_{HH} = 7.2$); 6.48 (t, 1H, C_6H_4Cl, $^3J_{HH} = 7.4$); 7.25–7.70 (m, 30H, PPh_3).
$Ru(C_6H_4Br\text{-}2)Cl(CO)(PPh_3)_2$ (**1b**)	5.46 (d, 1H, C_6H_4Br, $^3J_{HH} = 7.4$); 6.07 (t, 1H, C_6H_4Br, $^3J_{HH} = 7.1$); 6.34–6.42 (m, 2H, C_6H_4Br); 7.20–7.78 (m, 30H, PPh_3).
$Os(C_6H_4Cl\text{-}2)Cl(CO)(PPh_3)_2$ (**2a**)	5.60 (d, 1H, C_6H_4Cl, $^3J_{HH} = 7.3$); 6.14 (d, 1H, C_6H_4Cl, $^3J_{HH} = 6.9$); 6.19 (t, 1H, C_6H_4Cl, $^3J_{HH} = 7.3$); 6.41 (t, 1H, C_6H_4Cl, $^3J_{HH} = 7.5$); 7.24–7.61 (m, 30H, PPh_3)
$Os(C_6H_4Br\text{-}2)Cl(CO)(PPh_3)_2$ (**2b**)	5.40 (d, 1H, C_6H_4Br, $^3J_{HH} = 7.4$); 6.12 (t, 1H, C_6H_4Br, $^3J_{HH} = 7.1$); 6.22 (d, 1H, C_6H_4Br, $^3J_{HH} = 7.4$); 6.35 (t, 1H, C_6H_4Br, $^3J_{HH} = 7.4$); 7.26–7.70 (30H, m, PPh_3).
$Os(C_6H_4I\text{-}2)Cl(CO)(PPh_3)_2$ (**2c**)	5.22 (d, 1H, C_6H_4I, $^3J_{HH} = 7.3$); 5.99 (t, 1H C_6H_4I, $^3J_{HH} = 7.2$); 6.19 (t, 1H C_6H_4I, $^3J_{HH} = 7.3$); 6.38 (d, 1H, C_6H_4I, $^3J_{HH} = 7.8$); 6.95–7.70 (m, 30H, PPh_3).
$Ru(C_6H_4Br\text{-}2)(\eta^2\text{-}O_2CCH_3)(CO)(PPh_3)_2$ (**3**)	0.62 (s, 3H, CH_3CO_2); 6.27 (t, 1H, C_6H_4Br, $^3J_{HH} = 6.9$); 6.55 (t, 1H, C_6H_4Br, $^3J_{HH} = 6.8$); 6.72 (d, 1H, C_6H_4Br, $^2J_{HH} = 6.6$); 7.61 (t, d, C_6H_4Br, $^3J_{HH} = 7.0$); 7.17–7.43 (30H, m, PPh_3).
$Os(C_6H_4Br\text{-}2)(\eta^2\text{-}O_2CCH_3)(CO)(PPh_3)_2$ (**4**)	0.53 (s, 3H, CH_3CO_2); 6.24 (t, 1H, C_6H_4Br, $^3J_{HH} = 7.0$); 6.55 (t, 1H, C_6H_4Br $^3J_{HH} = 6.9$, $^4J_{HH} = 1.1$); 6.75 (d, 1H, C_6H_4Br, $^3J_{HH} = 7.9$, $^4J_{HH} = 1.4$); 7.28–7.46 (30H, m, PPh_3).
$Ru(C_6H_4Cl\text{-}2)Cl(CO)_2(PPh_3)_2$ (**5a**)	6.34 (t, 1H, C_6H_4Cl, $^3J_{HH} = 7.0$); 6.69 (t, 1H, C_6H_4Cl, $^3J_{HH} = 7.0$); 6.84 (d, 1H, C_6H_4Cl, $^3J_{HH} = 7.8$); 7.18 (d, 1H, C_6H_4Cl, $^3J_{HH} = 7.8$); 7.17–7.46 (m, 30H, PPh_3).
$Ru(C_6H_4Br\text{-}2)Cl(CO)_2(PPh_3)_2$ (**5b**)	6.42 (t, 1H, C_6H_4Br, $^3J_{HH} = 7.0$); 6.54 (t, 1H, C_6H_4Br, $^3J_{HH} = 7.6$); 6.81 (dd, 1H, C_6H_4Br, $^3J_{HH} = 7.8$, $^4J_{HH} = 1.6$); 6.88 (d, 1H, C_6H_4Br, $^3J_{HH} = 7.8$); 7.24–7.48 (m, 30H, PPh_3).
$Os(C_6H_4Cl\text{-}2)Cl(CO)_2(PPh_3)_2$ (**6a**)	6.36 (t, 1H, C_6H_4Cl, $^3J_{HH} = 7.1$); 6.68 (t, 1H, C_6H_4Cl, $^3J_{HH} = 7.1$); 6.83 (d, 1H, C_6H_4Cl, $^3J_{HH} = 7.7$); 7.15 (d, 1H, C_6H_4Cl, $^2J_{HH} = 7.7$); 7.14–7.45 (m, 30H, PPh_3).
$Os(C_6H_4Br\text{-}2)Cl(CO)_2(PPh_3)_2$ (**6b**)	6.35 (td, 1H, C_6H_4Br, $^3J_{HH} = 7.1$, $^4J_{HH} = 1.26$); 6.58 (t, 1H, C_6H_4Br, $^3J_{HH} = 7.4$); 7.05 (d, 1H, C_6H_4Br, $^3J_{HH} = 7.8$); 7.27 (dd, 1H, C_6H_4Br, $^3J_{HH} = 7.7$, $^4J_{HH} = 1.7$); 7.30–7.53 (m, 30H, PPh_3).
$Os(C_6H_4I\text{-}2)Cl(CO)_2(PPh_3)_2$ (**6c**)	6.37 (m, 2H, C_6H_4I); 7.03 (m, 2H, C_6H_4I); 7.24–7.52 (m, 30H, PPh_3).
$Os(C_6H_4Cl\text{-}2)Cl(CS)(PPh_3)_2$ (**7a**)	5.90 (dd, 1H, C_6H_4Cl, $^3J_{HH} = 7.2$, $^4J_{HH} = 1.2$); 6.27 (dd, 1H, C_6H_4Cl, $^3J_{HH} = 7.8$, $^4J_{HH} = 1.2$); 6.37 (td, 1H, C_6H_4Cl, $^3J_{HH} = 7.4$, $^4J_{HH} = 1.2$; 6.50 (bt, 1H, C_6H_4Cl, $^3J_{HH} = 6.5$); 7.02–7.65 (30H, m, PPh_3).
$Os(C_6H_4Br\text{-}2)Cl(CS)(PPh_3)_2$ (**7b**)	5.69 (d, 1H, C_6H_4Br, $^3J_{HH} = 7.2$); 6.29 (t, 1H, C_6H_4Br, $^3J_{HH} = 6.3$); 6.40 (m, 2H, C_6H_4Br); 7.02–7.54 (30H, m, PPh_3).
$Os(C_6H_4Cl\text{-}2)Cl(CS)(CO)(PPh_3)_2$ (**8a**)	6.33 (td, 1H, C_6H_4Cl, $^3J_{HH} = 7.4$, $^4J_{HH} = 1.3$); 6.68 (t, 1H, C_6H_4Cl, $^3J_{HH} = 6.6$); 6.83 (dd, 1H, C_6H_4Cl, $^3J_{HH} = 7.9$, $^4J_{HH} = 1.8$); 7.00 (dd, 1H, C_6H_4Cl, $^3J_{HH} = 7.8$, $^4J_{HH} = 1.2$); 6.37–6.44 (m, 2H, C_6H_4Cl); 7.25–7.57 (30H, m, PPh_3).
$Os(C_6H_4Br\text{-}2)Cl(CS)(CO)(PPh_3)_2$ (**8b**)	6.31 (td, 1H, C_6H_4Br, $^3J_{HH} = 7.4$, $^4J_{HH} = 1.3$); 6.57 (t, 1H, C_6H_4Br, $^3J_{HH} = 6.6$); 6.93 (dd, 1H, C_6H_4Br, $^3J_{HH} = 7.9$, $^4J_{HH} = 1.8$); 7.04 (dd, 1H, C_6H_4Br, $^3J_{HH} = 7.8$, $^4J_{HH} = 1.2$); 6.37–6.44 (m, 2H, C_6H_4Br); 7.22–7.69 (30H, m, PPh_3).
$Os(\eta^2\text{-}C[S]C_6H_4Cl\text{-}2)Cl(CO)(PPh_3)_2$ (**9a**)	6.71 (t, 1H, C_6H_4Cl, $^3J_{HH} = 7.3$, $^4J_{HH} = 0.8$); 6.96 (d, 1H, C_6H_4Cl, $^3J_{HH} = 7.5$); 7.21–7.72 (m, 2H, C_6H_4Cl, 30H, PPh_3).
$Os(\eta^2\text{-}C[S]C_6H_4Br\text{-}2)Cl(CO)(PPh_3)_2$ (**9b**)	6.76 (t, $^3J_{HH} = 7.2$, 1H, C_6H_4Br); 7.11 (t, 1H, C_6H_4Br, $^3J_{HH} = 7.2$); 7.15–7.88 (m, 32H, C_6H_4Br, PPh_3).
$Os(\eta^2\text{-}C[S]C_6H_4Sn^nBu_3\text{-}2)Cl(CO)(PPh_3)_2$ (**10**)	0.76 (t, 2H, $CH_3CH_2CH_2CH_2$, $^3J_{HH} = 8.1$); 0.83 (m, 3H, $CH_3CH_2CH_2CH_2$, $^3J_{HH} = 7.2$); 1.12–1.21 (m, 2H, $CH_3CH_2CH_2CH_2$); 1.27–1.34 (2H, $CH_3CH_2CH_2CH_2$); 6.75 (t, $^3J_{HH} = 7.2$, 1H, C_6H_4); 6.83 (t, 1H, C_6H_4 $^3J_{HH} = 7.8$); 7.20–7.64 (m, C_6H_4, PPh_3)

veals that **8a** is very similar to **6a**, with the thiocarbonyl ligand and the *o*-chlorophenyl ligands *cis* to one another.

2.4. Migratory insertion reactions of *8a* and *8b*

Aryl, thiocarbonyl complexes of osmium that are closely related to **8a** and **8b**, readily undergo migratory insertion to form η^2-thioacyl complexes [9]. For $Os(C_6H_4Me\text{-}4)Cl(CO)(CS)(PPh_3)_2$ this rearrangement occurs rapidly at room temperature (r.t.). In contrast, for **8a** and **8b** migratory insertion occurs only on heating under reflux in toluene to give the red–purple η^2-thioacyl complexes, $Os(\eta^2\text{-}C[S]C_6H_4X\text{-}2)Cl(CO)(PPh_3)_2$ (**9a** X = Cl; **9b** X = Br). While halogen substitution in the phenyl ring slows migration in these examples, it remains to be seen whether or not this is a general observation. Crystal structure determinations on both **9a** and **9b** have been obtained. The compounds are isostructural and a molecular geometry diagram for **9a** appears in Fig. 6 and selected bond distances and angles for **9a** and **9b** appear in Tables 10 and 11, respectively. The structures confirm the η^2-thioacyl geometry and bond distances and angles are as expected. The *o*-halophenyl ligands lie in the equatorial plane of the complexes and the halogen substituents, through being more remote from the metal centre, are less encumbered sterically than the same substituents in **8a** and **8a** (see Section 2.7).

Table 3
^{13}C-NMR data for *o*-halophenyl ruthenium(II) and osmium(II) complexes

Complex	Chemical shift (ppm)/Coupling constant (Hz)
Ru(C$_6$H$_4$Cl-2)Cl(CO)(PPh$_3$)$_2$ (**1a**)	122.22 (s, *C*$_6$H$_4$Cl); 123.74 (s, *C*$_6$H$_4$Cl); 127.84 (s, *C*$_6$H$_4$Cl); 139.02 (s, *C*$_6$H$_4$Cl); 155.2 (t, *C*$_6$H$_4$Cl C$_q$, $^2J_{CP} = 9.0$); 207.7 (*C*O, t, $^2J_{CP} = 17.6$); 128.25 (t′ [10], PPh$_3$ *ortho*, $^{2,4}J_{CP} = 10.1$); 130.17 (s, PPh$_3$ *para*); 132.65, (t′, PPh$_3$ *ipso*, $^{1,3}J_{CP} = 44.3$); 134.75 (t′, PPh$_3$ *meta*, $^{3,5}J_{CP} = 10.1$).
Ru(C$_6$H$_4$Br-2)Cl(CO)(PPh$_3$)$_2$ (**1b**)	122.11 (s, *C*$_6$H$_4$Br); 125.16 (s, *C*$_6$H$_4$Br); 139.20 (s, *C*$_6$H$_4$Br); 127.73 (t′, PPh$_3$ *ortho*, $^{2,4}J_{CP} = 9.1$); 129.54 (s, PPh$_3$ *para*); 132.59 (t′, PPh$_3$ *ipso*, $^{1,3}J_{CP} = 45.3$); 134.19 (t′, PPh$_3$ *meta*, $^{3,5}J_{CP} = 11.1$).
Os(C$_6$H$_4$Cl-2)Cl(CO)(PPh$_3$)$_2$ (**2a**)	121.4 (s, *C*$_6$H$_4$Cl); 123.86 (s, *C*$_6$H$_4$Cl); 127.93 (s, *C*$_6$H$_4$Cl); 138.43 (s, *C*$_6$H$_4$Cl); 179.38 (t, *C*O, $^2J_{CP} = 11.0$); 128.28 (t′, PPh$_3$ *ortho*, $^{2,4}J_{CP} = 9.1$); 130.25 (s, PPh$_3$ *para*); 132.36 (t′, PPh$_3$ *ipso*, $^{1,3}J_{CP} = 51.3$); 134.84 (t′, PPh$_3$ *meta*, $^{3,5}J_{CP} = 10.1$).
Os(C$_6$H$_4$Br-2)Cl(CO)(PPh$_3$)$_2$ (**2b**)	121.10 (s, *C*$_6$H$_4$Br); 125.22 (s, *C*$_6$H$_4$Br); 127.88 (s, *C*$_6$H$_4$Br); 131.63 (s, *C*$_6$H$_4$Br C$_q$); 138.57 (s, *C*$_6$H$_4$Br); 179.29 (t, $^2J_{CP} = 11.0$, *C*O); 127.71 (t′, PPh$_3$ *ortho*, $^{2,4}J_{CP} = 9.1$), 129.60 (s, PPh$_3$ *para*); 132.30 (t, PPh$_3$ *ipso*, $^{1,3}J_{CP} = 44.3$); 134.27 (t′, PPh$_3$ *meta*, $^{3,5}J_{CP} = 11.1$).
Os(C$_6$H$_4$I-2)Cl(CO)(PPh$_3$)$_2$ (**2c**)	109.32 (s, C$_q$); 121.99 (s, *C*$_6$H$_4$I); 128.79 (s, *C*$_6$H$_4$I); 129.55 (s, *C*$_6$H$_4$I); 140.54 (s, *C*$_6$H$_4$I); 134.77 (t, *C*$_6$H$_4$I C$_q$, $^2J_{CP} = 5.0$); 180.70 (t, *C*O, $^2J_{CP} = 11.0$); 128.17 (t′, PPh$_3$ *ortho*, $^{2,4}J_{CP} = 9.1$); 130.0 (s, PPh$_3$ *para*); 133.65 (t′ PPh$_3$ *ipso*, $^{1,3}J_{CP} = 50.3$); 134.77 (t′, PPh$_3$ *meta*, $^{3,5}J_{CP} = 10.1$).
Ru(C$_6$H$_4$Br-2)(η^2-O$_2$CCH$_3$)(CO)(PPh$_3$)$_2$ (**3**)	22.64 (s, *C*H$_3$CO$_2$); 122.41 (s, *C*$_6$H$_4$Br); 122.75 (s, *C*$_6$H$_4$Br); 132.68 (s, *C*$_6$H$_4$Br); 162.68 (t, *C*$_6$H$_4$Br C$_q$, $^2J_{CP} = 13.9$); 183.6 (s, CH$_3$*C*O$_2$); 208.71 (*C*O, t, $^2J_{CP} = 14.1$); 128.18 (t′, PPh$_3$ *ortho*, $^{2,4}J_{CP} = 9.1$); 130.00 (s, PPh$_3$); 131.37 (t′, PPh$_3$ *ipso*, $^{1,3}J_{CP} = 43.3$); 134.89 (t′, PPh$_3$ *meta*, $^{3,5}J_{CP} = 11.1$).
Os(C$_6$H$_4$Br-2)(η^2-O$_2$CCH$_3$)(CO)(PPh$_3$)$_2$ (**4**)	23.20 (s, *C*H$_3$CO$_2$); 121.29 (s, *C*$_6$H$_4$Br); 122.11 (s, *C*$_6$H$_4$Br); 131.86 (s, *C*$_6$H$_4$Br); 133.91 (s, *C*$_6$H$_4$Br); 142.34 (s, *C*$_6$H$_4$Br C$_q$); 142.60 (t, *C*$_6$H$_4$Br C$_q$, $^2J_{CP} = 13.7$); 184.18 (t, *C*O, $^2J_{CP} = 10.1$); 184.28 (s, CH$_3$*C*O$_2$); 127.69 (t′, PPh$_3$ *ortho*, $^{2,4}J_{CP} = 9.1$); 129.65 (s, PPh$_3$ *para*); 130.44 (t′, PPh$_3$ *ipso*, $^{1,3}J_{CP} = 49.3$); 134.51 (t′, PPh$_3$ *meta*, $^{3,5}J_{CP} = 10.1$).
Ru(C$_6$H$_4$Cl-2)Cl(CO)$_2$(PPh$_3$)$_2$ (**5a**)	124.56 (s, *C*$_6$H$_4$Cl); 125.28 (s, *C*$_6$H$_4$Cl); 127.83 (s, *C*$_6$H$_4$Cl); 144.31 (s, *C*$_6$H$_4$Cl); 158.81 (t, $^2J_{CP} = 11.0$); 194.66 (t, *C*O, $^2J_{CP} = 13.0$); 199.33 (t, *C*O, $^2J_{CP} = 13.0$); 128.08 (t′, PPh$_3$ *ortho*, $^{2,4}J_{CP} = 9.1$); 130.50 (s, PPh$_3$ *para*); 132.32 (t′, PPh$_3$ *ipso*, $^{1,3}J_{CP} = 46.3$); 134.96 (t′, PPh$_3$ *meta*, $^{3,5}J_{CP} = 10.1$).
Ru(C$_6$H$_4$Br-2)Cl(CO)$_2$(PPh$_3$)$_2$ (**5b**)	124.11 (s, *C*$_6$H$_4$Br); 125.11 (s, *C*$_6$H$_4$Br); 131.41 (s, *C*$_6$H$_4$Br); 143.64 (s, *C*$_6$H$_4$Br); 195.90 (t, *C*O, $^2J_{CP} = 17.0$); 202.78 (t, *C*O, $^2J_{CP} = 17.0$); 128.12 (t′, PPh$_3$ *ortho*, $^{2,4}J_{CP} = 12.1$); 130.52 (s, PPh$_3$ *para*); 132.01 (t′, PPh$_3$ *ipso*, $^{1,3}J_{CP} = 46.3$); 134.85 (t′, PPh$_3$ *meta*, $^{3,5}J_{CP} = 11.1$).
Os(C$_6$H$_4$Cl-2)Cl(CO)$_2$(PPh$_3$)$_2$ (**6a**)	124.42 (s, *C*$_6$H$_4$Cl); 124.78 (s, *C*$_6$H$_4$Cl); 127.29 (s, *C*$_6$H$_4$Cl); 143.76 (s, *C*$_6$H$_4$Cl); 148.17 (s, *C*$_6$H$_4$Cl C$_q$); 150.05 (t, *C*$_6$H$_4$Cl C$_q$, $^2J_{CP} = 10.1$); 177.95 (t, *C*O, $^2J_{CP} = 8.1$); 180.52 (t, *C*O, $^2J_{CP} = 7.0$); 127.5 (t′, PPh$_3$ *ortho*, $^{2,4}J_{CP} = 10.1$); 130.12 (s, PPh$_3$); 130.94 (t, PPh$_3$ *ipso*, $^{1,3}J_{CP} = 52.3$); 134.5 (t′, PPh$_3$ *meta*, $^{3,5}J_{CP} = 10.1$).
Os(C$_6$H$_4$Br-2)Cl(CO)$_2$(PPh$_3$)$_2$ (**6b**)	125.02 (s, *C*$_6$H$_4$Br); 125.28 (s, *C*$_6$H$_4$Br); 131.68 (s, *C*$_6$H$_4$Br); 144.74 (s, *C*$_6$H$_4$Br); 148.28 (s, *C*$_6$H$_4$Br C$_q$); 153.39 (t, C$_q$ *C*$_6$H$_4$Br, $^2J_{CP} = 11.1$); 178.63 (t, *C*O, $^2J_{CP} = 9.1$); 180.28 (t, *C*O, $^2J_{CP} = 6.0$); 127.56 (t′, PPh$_3$ *ortho*, $^{2,4}J_{CP} = 11.1$); 130.22 (s, PPh$_3$ *para*); 130.98 (t′, PPh$_3$ *ipso*, $^{1,3}J_{CP} = 42.3$); 134.73 (t′, PPh$_3$ *meta*, $^{3,5}J_{CP} = 9.1$).
Os(C$_6$H$_4$I-2)Cl(CO)$_2$(PPh$_3$)$_2$ (**6c**)	125.28 (s, *C*$_6$H$_4$I); 125.57 (s, *C*$_6$H$_4$I); 140.09 (s, *C*$_6$H$_4$I); 145.77 (s, *C*$_6$H$_4$I); 180.19 (t, *C*O, $^2J_{CP} = 17.0$); 180.25 (t, *C*O, $^2J_{CP} = 17.0$); 127.99 (t′, PPh$_3$ *ortho*, $^{2,4}J_{CP} = 9.1$); 130.69 (s, PPh$_3$ *para*); 131.32 (t, PPh$_3$ *ipso*, $^{1,3}J_{CP} = 53.3$); 135.37 (t′, PPh$_3$ *meta*, $^{3,5}J_{CP} = 9.1$).
Os(C$_6$H$_4$Cl-2)Cl(CS)(PPh$_3$)$_2$ (**7a**)	122.71 (s, *C*$_6$H$_4$Cl); 124.44 (s, *C*$_6$H$_4$Cl); 127.79 (s, *C*$_6$H$_4$Cl); 136.82 (s, *C*$_6$H$_4$Cl); 127.59 (t′, PPh$_3$ *ortho*, $^{2,4}J_{CP} = 9.1$); 129.87 (s, PPh$_3$ *para*); 130.79 (t′, PPh$_3$ *ipso*, $^{1,3}J_{CP} = 52.3$); 134.71 (t′, PPh$_3$ *meta*, $^{3,5}J_{CP} = 10.1$).
Os(C$_6$H$_4$Br-2)Cl(CS)(PPh$_3$)$_2$ (**7b**)	122.52 (s, *C*$_6$H$_4$Br); 125.91 (s, *C*$_6$H$_4$Br); 128.36 (s, *C*$_6$H$_4$Br); 136.48 (s, *C*$_6$H$_4$Br); 138.66 (s, *C*$_6$H$_4$Br C$_q$); 139.82 (t, *C*$_6$H$_4$Br C$_q$, $^2J_{CP} = 11.0$); 224.92 (t, *C*S, $^2J_{CP} = 13.2$); 127.55 (t′, PPh$_3$ *ortho*, $^{2,4}J_{CP} = 9.1$); 131.27 (t′, PPh$_3$ *ipso*, $^{1,3}J_{CP} = 46.3$); 134.70 (t′, PPh$_3$ *meta*, $^{3,5}J_{CP} = 10.1$).
Os(C$_6$H$_4$Cl-2)Cl(CS)(CO)(PPh$_3$)$_2$ (**8a**)	124.39 (s, *C*$_6$H$_4$Cl); 124.87 (s, *C*$_6$H$_4$Cl); 127.76 (s, *C*$_6$H$_4$Cl); 144.03 (s, *C*$_6$H$_4$Cl); 149.63 (s, *C*$_6$H$_4$Cl C$_q$); 150.84 (t, *C*$_6$H$_4$Cl C$_q$, $^2J_{CP} = 11.1$); 181.69 (t, *C*O, $^2J_{CP} = 7.0$); 127.31 (t′, PPh$_3$ *ortho*, $^{2,4}J_{CP} = 10.1$); 130.17 (s, PPh$_3$ *para*); 130.31 (t′, PPh$_3$ *ipso*, $^{1,3}J_{CP} = 52.3$); 134.90 (t′, PPh$_3$ *meta*, $^{3,5}J_{CP} = 9.1$).
Os(C$_6$H$_4$Br-2)Cl(CS)(CO)(PPh$_3$)$_2$ (**8b**)	124.66 (s, *C*$_6$H$_4$Br); 124.98 (s, *C*$_6$H$_4$Br); 131.94 (s, *C*$_6$H$_4$Br); 144.90 (s, *C*$_6$H$_4$Br); 143.85 (s, *C*$_6$H$_4$Br C$_q$); 153.72 (t, *C*$_6$H$_4$Br C$_q$, $^2J_{CP} = 11.1$); 181.26 (t, *C*O, $^2J_{CP} = 6.0$); 127.30 (t′, PPh$_3$ *ortho*, $^{2,4}J_{CP} = 10.1$); 130.19 (s, PPh$_3$ *para*); 130.30 (t, PPh$_3$ *ipso*, $^{1,3}J_{CP} = 54.3$); 135.02 (t, PPh$_3$ *meta* $^{3,5}J_{CP} = 10.1$).
Os(η^2-C[S]C$_6$H$_4$Cl-2)Cl(CO)(PPh$_3$)$_2$ (**9a**)	126.58 (s, *C*$_6$H$_4$Cl); 130.49 (s, *C*$_6$H$_4$Cl), 131.22 (s, *C*$_6$H$_4$Cl); 139.63 (s, *C*$_6$H$_4$Cl C$_q$); 139.70 (s, *C*$_6$H$_4$Cl); 127.68 (t′, PPh$_3$ *ortho*, $^{2,4}J_{CP} = 9.1$); 129.82 (s, PPh$_3$); 131.28 (t, PPh$_3$ *ipso*, $^{1,3}J_{CP} = 51.3$); 134.15 (t′, PPh$_3$ *meta*, $^{3,5}J_{CP} = 10.1$).
Os(η^2-C[S]C$_6$H$_4$Br-2)Cl(CO)(PPh$_3$)$_2$ (**9b**)	127.66 (s, *C*$_6$H$_4$Br); 141.13 (s, *C*$_6$H$_4$Br); 190.81 (t, *C*O); 207.35 (t, *C*S); 128.24 (t′, PPh$_3$ *ortho*, $^{2,4}J_{CP} = 10.1$); 134,64 (t′, PPh$_3$ *meta*, $^{3,5}J_{CP} = 10.1$); 130.31 (s, PPh$_3$ *para*); 131.49 (t, PPh$_3$ *ipso*, $^{1,3}J_{CP} = 34.2$).
Os(η^2-C[S]C$_6$H$_4$Sn^{n}Bu$_3$-2)Cl(CO)(PPh$_3$)$_2$ (**10**)	12.49 (s, CH$_3$CH$_2$CH$_2$CH$_2$); 13.79 (s, CH$_3$CH$_2$CH$_2$CH$_2$); 27.20 (s, CH$_3$CH$_2$CH$_2$CH$_2$); 28.95 (s, CH$_3$CH$_2$CH$_2$CH$_2$); 128.06 (s, *C*$_6$H$_4$); 128.32 (s, *C*$_6$H$_4$); 137.47 (s, *C*$_6$H$_4$); 139.31 (s, *C*$_6$H$_4$); 143.73 (s, *C*$_6$H$_4$ C$_q$); 148.96 (t, *C*$_6$H$_4$ C$_q$, $^2J_{CP} = 12.07$); 190.67 (t, CO, $^2J_{CP} = 10.1$); 127.63 (t′, PPh$_3$ *ortho*, $^{2,4}J_{CP} = 9.1$); 129.8 (s, PPh$_3$ *para*); 130.94 (PPh$_3$ *ipso*, $^{1,3}J_{CP} = 50.3$); 134.24 (t′, PPh$_3$ *meta*, $^{3,5}J_{CP} = 10.04$).

Table 4
Data collection and processing parameters for **2a**–**c**, **6a**, **8a**, and **9a**–**b** [a]

	2a	**2b**	**2c**	**6a**	**8a**	**9a**	**9b**
Formula	$C_{43}H_{34}Cl_2OOsP_2$	$C_{43}H_{34}BrClOOsP_2$	$C_{43}H_{34}ClIOOsP_2$	$C_{44}H_{34}Cl_2O_2OsP_2$	$C_{44}H_{34}Cl_2OOsP_2S$	$C_{44}H_{34}Cl_2OOsP_2S$	$C_{44}H_{34}BrClOOsP_2S$
Molecular weight	889.74	934.20	981.19	917.75	933.81	933.81	978.27
Crystal system	Orthorhombic	Orthorhombic	Orthorhombic	Orthorhombic	Monoclinic	Monoclinic	Monoclinic
Space group	$Pca2_1$	$Pca2_1$	$Pca2_1$	$Pbca$	$P2_1/n$	$P2_1/n$	$P2_1/n$
Unit cell dimensions							
a (Å)	15.9510(2)	15.9460(2)	15.9886(1)	11.8750(1)	9.8873(3)	11.7180(1)	11.7036(5)
b (Å)	13.9165(1)	13.8543(3)	13.8528(1)	17.6310(3)	34.5933(11)	14.9819(2)	15.1154(6)
c (Å)	16.8663(3)	16.7656(3)	16.7844(1)	35.1581(5)	11.8654(4)	21.6774(3)	21.5949(9)
β (°)					109.589(1)	98.438(1)	98.427(1)
V (Å^3)	3744.02(9)	3703.87(11)	3717.52(6)	7360.92(16)	3823.5(2)	3764.31(3)	3779.0(3)
Z	4	4	4	8	4	4	4
D_{calc} (g cm^{-3})	1.578	1.675	1.753	1.656	1.622	1.648	1.719
F(000)	1760	1832	1904	3632	1848	1848	1920
μ (mm^{-1})	3.66	4.71	4.45	3.73	3.64	3.71	4.68
2θ (min–max) (°)	1.5–24.0	1.5–28	1.5–28	2.1–26	1.2–28	1.6–28	2.2–28
Unique reflections	4618	7408	4444	7232	8620	8781	8533
No. of observed reflections [$I>2\sigma(I)$]	3876	6719	4049	6528	6123	7950	7621
Crystal size (mm)	0.25 × 0.22 × 0.20	0.26 × 0.18 × 0.12	0.30 × 0.21 × 0.18	0.37 × 0.17 × 0.15	0.42 × 0.05 × 0.05	0.40 × 0.18 × 0.08	0.32 × 0.18 × 0.12
A (min–max)	0.461 0.527	0.373 0.602	0.348 0.501	0.338 0.604	0.309 0.838	0.319 0.756	0.316 0.604
No. of variables in LS	442	442	442	460	460	461	461
Goodness-of-fit on F^2	1.195	0.936	1.030	1.427	1.126	1.081	1.051
R (observed data)	0.0442	0.0334	0.0286	0.0524	0.0528	0.0220	0.0274
wR_2 (all data)	0.1162	0.0861	0.0701	0.0934	0.0821	0.0527	0.0844
Difference map (min–max) (e Å^{-3})	−0.96 +0.88	−0.77 +0.95	−1.52 +1.09	−2.00 +1.50	−1.26 +1.12	−0.65 +1.49	−1.62 +1.62

[a] Siemens SMART area detector using graphite monochromated Mo–K$_\alpha$, $\lambda = 0.71073$. Function minimised. $\Sigma\, w(F_o^2 - F_c^2)^2$. $R = \Sigma\|F_o| - |F_c\|/\Sigma|F_o|$. $wR_2 = \{\Sigma[w(F_o^2 - F_c^2)^2]/\Sigma[w(F_o^2)^2]\}^{1/2}$.

Table 5
Selected bond lengths (Å) and angles (°) for **2a**

Bond lengths	
Os–C(1)	1.850(19)
Os–C(2)	2.060(16)
Os–P(1)	2.388(4)
Os–P(2)	2.401(3)
Os–Cl(1)	2.466(4)
Os–Cl(2)	2.826(4)
Cl(2)–C(3)	1.817(17)
O(1)–C(1)	1.062(18)
C(2)–C(7)	1.344(19)
C(2)–C(3)	1.39(2)
C(3)–C(4)	1.32(3)
C(4)–C(5)	1.40(3)
C(5)–C(6)	1.42(3)
C(6)–C(7)	1.46(2)
Bond angles	
C(1)–Os–C(2)	94.2(6)
C(1)–Os–P(1)	88.8(5)
C(2)–Os–P(1)	92.6(4)
C(1)–Os–P(2)	89.9(5)
C(2)–Os–P(2)	91.7(4)
P(1)–Os–P(2)	175.58(13)
C(1)–Os–Cl(1)	112.6(5)
C(2)–Os–Cl(1)	153.1(5)
P(1)–Os–Cl(1)	86.56(13)
P(2)–Os–Cl(1)	90.05(12)
C(1)–Os–Cl(2)	157.2(5)
C(2)–Os–Cl(2)	63.1(5)
P(1)–Os–Cl(2)	94.05(13)
P(2)–Os–Cl(2)	88.79(13)
Cl(1)–Os–Cl(2)	90.18(13)
C(3)–Cl(2)–Os	73.7(6)
O(1)–C(1)–Os	175.2(15)
C(7)–C(2)–Os	129.6(13)
C(3)–C(2)–Os	113.1(12)
C(4)–C(3)–Cl(2)	118.4(15)
C(2)–C(3)–Cl(2)	110.1(12)

2.5. *o*-Halophenyl complexes as potential precursors of benzyne complexes

Based on the route to benzyne complexes established by Bennett et al. [3] the compounds **1**, **2**, **5**, **6**, **7**, and **8** appeared to be ideal precursors to both coordinatively unsaturated, **11**, and coordinatively saturated benzyne complexes, **12**, as shown in Scheme 3. Unfortunately, all attempts at reduction, whether beginning with the five coordinate or six coordinate *o*-halophenyl complexes were unsuccessful. In the case of the five coordinate, starting materials reactions occurred but no tractable products could be isolated, and in the case of the six coordinate starting materials, no reaction was observed. The reducing reagents investigated included, ^{n}BuLi, ^{t}BuLi, 1–5% Na/Hg amalgam, activated zinc, and activated magnesium.

2.6. Lithiation of $Os(\eta^2\text{-}C[S]C_6H_4Br\text{-}2)Cl(CO)(PPh_3)_2$ (**9b**)

Despite the lack of reactivity shown by the *o*-halo-substituent in the saturated *o*-halophenyl complexes, **5**, **6**, and **8**, lithiation occurs readily once the *o*-halophenyl group is removed from the metal as in the migrated product **9b**. Treatment of a red–purple solution of $Os(\eta^2\text{-}C[S]C_6H_4Br\text{-}2)Cl(CO)(PPh_3)_2$ (**9b**) with one molar equivalent of ^{n}BuLi resulted in an immediate colour change to bright orange. Quenching this orange solution by the addition of excess MeI gave a dark red mixture of $Os(\eta^2\text{-}C[S]C_6H_4Me\text{-}2)Cl(CO)(PPh_3)_2$ and $Os(\eta^2\text{-}C[S]C_6H_5)Cl(CO)(PPh_3)_2$ as confirmed by FAB$^+$ mass spectroscopy. When the reaction was repeated using ^{n}Bu$_3$SnCl as the quenching electrophile, red–purple crystals of $Os(\eta^2\text{-}C[S]C_6H_4Sn^nBu_3\text{-}2)Cl(CO)(PPh_3)_2$ (**10**) were isolated and characterised (see Scheme 2).

Table 6
Selected bond lengths (Å) and angles (°) for **2b**

Bond lengths	
Os–C(1)	1.807(7)
Os–C(2)	2.038(7)
Os–P(2)	2.3824(17)
Os–P(1)	2.4017(17)
Os–Cl	2.4675(16)
Os–Br	2.8323(8)
Br–C(3)	1.930(7)
O(1)–C(1)	1.152(9)
C(2)–C(7)	1.392(9)
C(2)–C(3)	1.391(10)
C(3)–C(4)	1.384(10)
C(4)–C(5)	1.397(13)
C(5)–C(6)	1.383(14)
C(6)–C(7)	1.447(11)
Bond angles	
C(1)–Os–C(2)	91.6(3)
C(1)–Os–P(2)	88.7(2)
C(2)–Os–P(2)	92.5(2)
C(1)–Os–P(1)	89.2(2)
C(2)–Os–P(1)	93.2(2)
P(2)–Os–P(1)	173.97(6)
C(1)–Os–Cl	111.3(2)
C(2)–Os–Cl	157.0(2)
P(2)–Os–Cl	89.77(6)
P(1)–Os–Cl	85.75(6)
C(1)–Os–Br	158.0(2)
C(2)–Os–Br	66.5(2)
P(2)–Os–Br	89.72(4)
P(1)–Os–Br	94.37(4)
Cl–Os–Br	90.60(4)
C(3)–Br–Os	71.0(2)
O(1)–C(1)–Os	178.5(7)
C(7)–C(2)–Os	132.2(5)
C(3)–C(2)–Os	111.7(5)
C(4)–C(3)–Br	122.3(6)
C(2)–C(3)–Br	110.8(5)

Table 7
Selected bond lengths (Å) and angles (°) for **2c**

Bond lengths	
Os–C(1)	1.794(8)
Os–C(2)	2.105(8)
Os–P(1)	2.3770(18)
Os–P(2)	2.4007(18)
Os–Cl	2.4672(18)
Os–I	2.9335(6)
I–C(3)	2.125(7)
O(1)–C(1)	1.127(10)
C(2)–C(7)	1.370(10)
C(2)–C(3)	1.395(10)
C(3)–C(4)	1.380(11)
C(4)–C(5)	1.411(13)
C(5)–C(6)	1.383(13)
C(6)–C(7)	1.417(10)
Bond angles	
C(1)–Os–C(2)	90.3(3)
C(1)–Os–P(1)	89.7(2)
C(2)–Os–P(1)	93.9(2)
C(1)–Os–P(2)	88.8(2)
C(2)–Os–P(2)	91.2(2)
P(1)–Os–P(2)	174.71(6)
C(1)–Os–Cl	110.7(3)
C(2)–Os–Cl	159.0(2)
P(1)–Os–Cl	86.54(6)
P(2)–Os–Cl	89.27(6)
C(1)–Os–I	158.6(3)
C(2)–Os–I	68.4(2)
P(1)–Os–I	93.74(4)
P(2)–Os–I	89.52(5)
Cl–Os–I	90.60(4)
C(3)–I–Os	68.91(19)
O(1)–C(1)–Os	177.4(7)
C(7)–C(2)–Os	131.1(5)
C(3)–C(2)–Os	112.6(5)
C(4)–C(3)–I	123.5(6)
C(2)–C(3)–I	110.1(5)

2.7. Summary

Sets of *o*-halophenyl derivatives of ruthenium(II) and osmium(II) have been prepared for the purpose of examining the potential of these compounds as precursors, through reduction, to ruthenium(0) and osmium(0) benzyne complexes. No routes to benzyne complexes were found using these starting materials, but it was established that when the *o*-halophenyl group is bound in coordinatively unsaturated complexes, there is a bonding interaction between the halogen substituent and the metal centre. When a thiocarbonyl ligand is presented adjacent to the *o*-halophenyl ligand, migratory insertion reactions ensue leading to η^2-thioacyl complexes. In the latter compounds, where the *o*-halophenyl group is no longer bound to the metal, normal organic reactivity returns to the halogen substituents as exemplified by ready lithiation and subsequent stannylation.

Table 8
Selected bond lengths (Å) and angles (°) for **6a**

Bond lengths	
Os–C(2)	1.917(8)
Os–C(1)	1.959(7)
Os–C(3)	2.169(6)
Os–P(1)	2.4142(14)
Os–Cl(1)	2.4295(17)
Os–P(2)	2.4365(15)
Cl(2)–C(4)	1.761(7)
C(1)–O(1)	1.080(8)
C(2)–O(2)	1.067(8)
C(3)–C(4)	1.388(9)
C(3)–C(8)	1.457(9)
C(4)–C(5)	1.386(10)
C(5)–C(6)	1.367(11)
C(6)–C(7)	1.372(11)
C(7)–C(8)	1.372(10)
Bond angles	
C(2)–Os–C(1)	87.8(3)
C(2)–Os–C(3)	94.9(2)
C(1)–Os–C(3)	177.2(2)
C(2)–Os–P(1)	87.18(19)
C(1)–Os–P(1)	92.46(19)
C(3)–Os–P(1)	88.10(16)
C(2)–Os–Cl(1)	176.30(19)
C(1)–Os–Cl(1)	88.58(18)
C(3)–Os–Cl(1)	88.71(17)
P(1)–Os–Cl(1)	92.26(6)
C(2)–Os–P(2)	96.13(19)
C(1)–Os–P(2)	87.97(19)
C(3)–Os–P(2)	91.32(16)
P(1)–Os–P(2)	176.68(5)
Cl(1)–Os–P(2)	84.46(6)
O(1)–C(1)–Os	175.4(6)
O(2)–C(2)–Os	172.5(6)
C(4)–C(3)–Os	130.1(5)
C(8)–C(3)–Os	118.1(4)
C(5)–C(4)–Cl(2)	113.7(5)
C(3)–C(4)–Cl(2)	120.4(5)

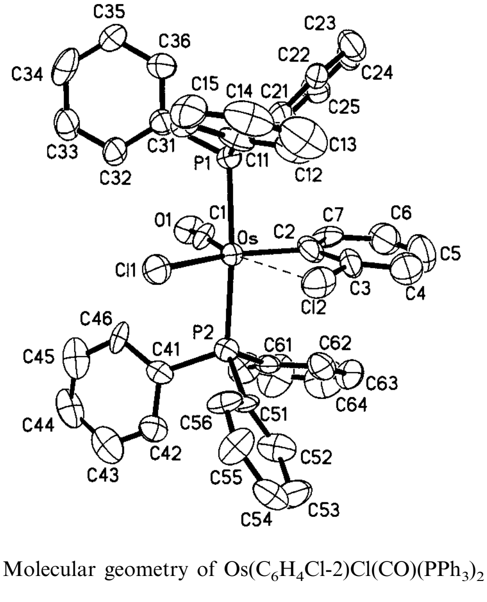

Fig. 2. Molecular geometry of $Os(C_6H_4Cl\text{-}2)Cl(CO)(PPh_3)_2$ (**2a**).

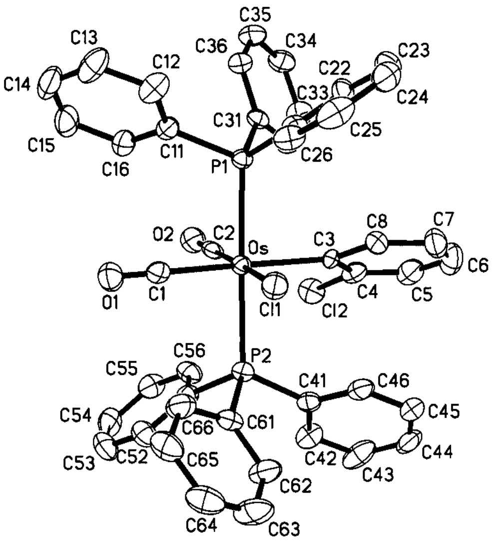

Fig. 3. Molecular geometry of $Os(C_6H_4Cl\text{-}2)Cl(CO)_2(PPh_3)_2$ (**6a**).

3. Experimental

3.1. General procedures and instruments

Standard laboratory procedures were followed as have been described previously [10]. The compounds $RuHCl(CO)(PPh_3)_3$ [11], $OsHCl(CO)(PPh_3)_3$ [12], $OsHCl(CS)(PPh_3)_3$ [13], $Hg(C_6H_4Cl\text{-}2)_2$ [6], $Hg(C_6H_4Br\text{-}2)_2$ [14], and $Hg(C_6H_4I\text{-}2)_2$ [15], were prepared according to literature methods.

Infrared spectra (4000–400 cm^{-1}) were recorded as Nujol mulls between KBr plates on a Perkin–Elmer Paragon 1000 spectrometer. NMR spectra were obtained on a Bruker DRX 400 at 25°C. ^1H- and ^{13}C-NMR spectra were obtained operating at 400.1 (^1H) or 100.6 (^{13}C) MHz, respectively. Resonances are quoted in ppm and ^1H-NMR spectra referenced to either tetramethylsilane (0.00 ppm) or the proteo-impurity in the solvent (7.25 ppm for $CHCl_3$). ^{13}C-NMR spectra were referenced to $CDCl_3$ (77.00 ppm). Mass spectra were recorded using the fast atom bombardment technique with a Varian VG 70-SE mass spectrometer. Melting points (uncorrected) were determined on a Reichert hot stage microscope. Elemental analyses were obtained from the Micro-analytical Laboratory, University of Otago.

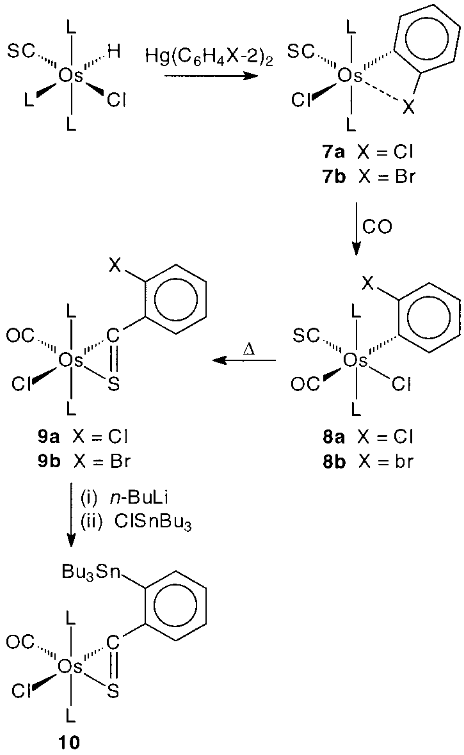

Scheme 2. Synthesis and reactions of the thiocarbonyl-containing *o*-halophenyl complexes, $Os(C_6H_4X\text{-}2)Cl(CS)(PPh_3)_2$.

	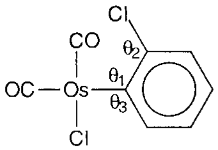	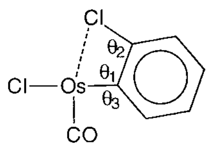		
		X = Cl	X = Br	X = I
Os–C (Å)	2.169(6)	2.060(16)	2.038(7)	2.105(8)
Os···X (Å)		2.826(4)	2.8323(8)	2.9335(6)
θ_1 (°)	130.1(5)	113.1(12)	111.7(5)	112.6(5)
θ_2 (°)	120.4(5)	110.1(12)	110.8(5)	110.1(5)
θ_3 (°)	118.1(4)	129.6(13)	132.2(5)	131.1(5)

Fig. 4. Selected structural data for five coordinate ($Os(C_6H_4X\text{-}2)Cl(CO)(PPh_3)_2$) and six coordinate ($Os(C_6H_4Cl\text{-}2)Cl(CO)_2(PPh_3)_2$) *o*-halophenyl complexes of osmium. (View down P–Os–P axis, PPh_3 ligands omitted for clarity.)

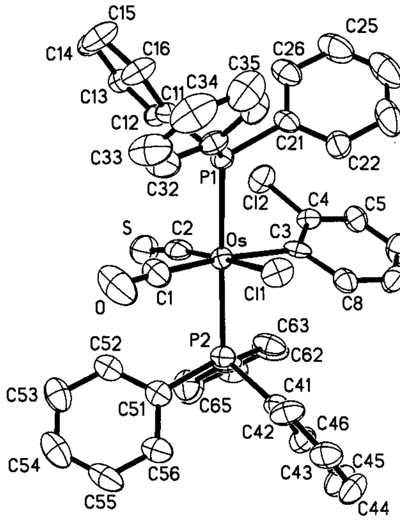

Fig. 5. Molecular geometry of Os(C$_6$H$_4$Cl-2)Cl(CO)(CS)(PPh$_3$)$_2$ (**8a**).

Table 9
Selected bond lengths (Å) and angles (°) for **8a**

Bond lengths	
Os–C(2)	1.872(7)
Os–C(1)	1.913(7)
Os–C(3)	2.169(6)
Os–P(2)	2.4492(14)
Os–P(1)	2.4521(14)
Os–Cl(1)	2.4895(16)
Cl(2)–C(4)	1.753(6)
S–C(2)	1.519(7)
O–C(1)	1.155(7)
C(3)–C(4)	1.414(7)
C(3)–C(8)	1.445(8)
C(4)–C(5)	1.382(8)
C(5)–C(6)	1.370(9)
C(6)–C(7)	1.380(8)
C(7)–C(8)	1.367(8)
Bond angles	
C(2)–Os–C(1)	92.6(3)
C(2)–Os–C(3)	95.2(2)
C(1)–Os–C(3)	171.4(3)
C(2)–Os–P(2)	84.66(19)
C(1)–Os–P(2)	89.36(19)
C(3)–Os–P(2)	87.86(14)
C(2)–Os–P(1)	97.57(19)
C(1)–Os–P(1)	90.39(19)
C(3)–Os–P(1)	92.06(14)
P(2)–Os–P(1)	177.76(6)
C(2)–Os–Cl(1)	176.0(2)
C(1)–Os–Cl(1)	83.4(2)
C(3)–Os–Cl(1)	88.72(16)
P(2)–Os–Cl(1)	94.96(5)
P(1)–Os–Cl(1)	82.81(5)
O–C(1)–Os	175.8(7)
S–C(2)–Os	173.6(4)
C(4)–C(3)–Os	130.8(5)
C(8)–C(3)–Os	118.3(4)
C(5)–C(4)–Cl(2)	113.2(5)
C(3)–C(4)–Cl(2)	121.1(5)

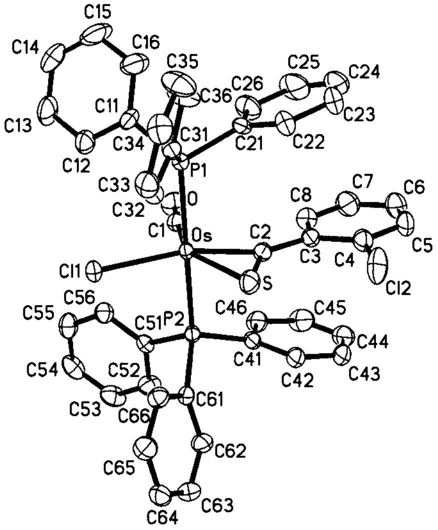

Fig. 6. Molecular geometry of Os(η^2-C[S]C$_6$H$_4$Cl-2)Cl(CO)(PPh$_3$)$_2$ (**9a**).

Table 10
Selected bond lengths (Å) and angles (°) for **9a**

Bond lengths	
Os–C(1)	1.857(3)
Os–C(2)	1.961(3)
Os–P(2)	2.4009(6)
Os–P(1)	2.4075(7)
Os–Cl(1)	2.4938(6)
Os–S	2.4989(7)
S–C(2)	1.695(3)
O–C(1)	1.175(3)
C(2)–C(3)	1.450(4)
C(3)–C(8)	1.389(4)
C(3)–C(4)	1.430(4)
C(4)–C(5)	1.386(4)
C(5)–C(6)	1.382(5)
C(6)–C(7)	1.392(5)
C(7)–C(8)	1.384(4)
Bond angles	
C(1)–Os–C(2)	106.75(12)
C(1)–Os–P(2)	89.15(9)
C(2)–Os–P(2)	89.79(8)
C(1)–Os–P(1)	88.19(9)
C(2)–Os–P(1)	90.31(8)
P(2)–Os–P(1)	177.26(2)
C(1)–Os–Cl(1)	103.76(9)
C(2)–Os–Cl(1)	149.50(8)
P(2)–Os–Cl(1)	90.66(2)
P(1)–Os–Cl(1)	90.64(2)
C(1)–Os–S	149.33(9)
C(2)–Os–S	42.59(8)
P(2)–Os–S	90.23(2)
P(1)–Os–S	91.70(2)
Cl(1)–Os–S	106.91(2)
C(2)–S–Os	51.51(9)
O–C(1)–Os	176.6(3)
C(3)–C(2)–Os	142.3(2)
S–C(2)–Os	85.90(12)
C(5)–C(4)–Cl(2)	116.7(3)
C(3)–C(4)–Cl(2)	121.9(2)

Table 11
Selected bond lengths (Å) and angles (°) for **9b**

Bond lengths	
Os–C(1)	1.854(4)
Os–C(2)	1.957(4)
Os–P(2)	2.3998(9)
Os–P(1)	2.4047(9)
Os–Cl	2.4942(9)
Os–S	2.4988(10)
Br–C(4)	1.889(5)
S–C(2)	1.696(4)
O–C(1)	1.159(5)
C(2)–C(3)	1.447(5)
C(3)–C(8)	1.401(6)
C(3)–C(4)	1.419(6)
C(4)–C(5)	1.385(6)
C(5)–C(6)	1.384(7)
C(6)–C(7)	1.402(7)
C(7)–C(8)	1.392(6)
Bond angles	
C(1)–Os–C(2)	107.23(17)
C(1)–Os–P(2)	89.41(12)
C(2)–Os–P(2)	89.74(10)
C(1)–Os–P(1)	88.44(12)
C(2)–Os–P(1)	90.24(10)
P(2)–Os–P(1)	177.74(3)
C(1)–Os–Cl	103.43(12)
C(2)–Os–Cl	149.33(12)
P(2)–Os–Cl	90.54(3)
P(1)–Os–Cl	90.64(3)
C(1)–Os–S	149.85(12)
C(2)–Os–S	42.61(12)
P(2)–Os–S	90.23(3)
P(1)–Os–S	91.28(3)
Cl–Os–S	106.72(3)
C(2)–S–Os	51.39(13)
O–C(1)–Os	175.9(4)
C(3)–C(2)–S	131.4(3)
C(3)–C(2)–Os	142.6(3)
S–C(2)–Os	86.00(17)
C(5)–C(4)–Br	116.1(4)
C(3)–C(4)–Br	122.2(3)

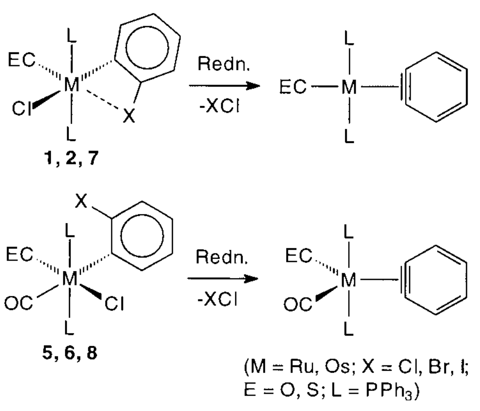

Scheme 3. Proposed synthetic routes to benzyne complexes.

3.2. *Ru(C_6H_4Cl-2)Cl(CO)(PPh_3)$_2$ (**1a**)*

$RuHCl(CO)(PPh_3)_3$ (200 mg, 0.210 mmol) and $Hg(C_6H_4Cl\text{-}2)_2$ (98 mg, 0.23 mmol) were heated under reflux in toluene for 24 h. The resulting yellow solution was cooled, and the toluene was removed in vacuo. The product was dissolved in dichloromethane (20 ml), filtered through a Celite pad to remove elemental mercury and ethanol (10 ml) was then added. Removal of the dichloromethane on a rotary evaporator yielded bright yellow crystals of **1a** (135 mg, 80%). M.p. 180–181°C. *m*/*z* 765; $C_{43}H_{34}ClOP_2Ru$ [$M^+ - C$] 765. Anal. Calc. for $C_{43}H_{34}Cl_2OP_2Ru \cdot 1/4CH_2Cl_2$: C, 63.22; H, 4.23. Found: C, 63.21; H, 4.29%.

3.3. *Ru(C_6H_4Br-2)Cl(CO)(PPh_3)$_2$ (**1b**)*

To a dichloromethane (10 ml) solution of Ru(C_6H_4Br-2)(η^2-O_2CCH_3)(CO)(PPh_3)$_2$ (**3**) (see Section 3.7) (50 mg, 0.0575 mmol), one drop of HCl (conc.) in EtOH (5 ml) was added. The resulting bright yellow solution was reduced in volume on the rotary evaporator and yellow crystals of **1b** were filtered off and collected (47 mg, 97%). *m*/*z* 844.0042; $C_{43}H_{34}OBrClRuP_2$ requires 844.0000. Anal. Calc. for $C_{43}H_{34}BrClRuOP_2 \cdot H_2O$: C, 59.84; H, 4.20. Found: C, 60.26; H, 4.17%.

3.4. *Os(C_6H_4Cl-2)Cl(CO)(PPh_3)$_2$ (**2a**)*

$OsHCl(CO)(PPh_3)_3$ (200 mg, 0.192 mmol) and $Hg(C_6H_4Cl\text{-}2)_2$ (90 mg, 0.21 mmol) were added to toluene (50 ml) and the mixture heated under reflux for 3 h. The resulting yellow solution was cooled, and the toluene was removed in vacuo. The product was dissolved in dichloromethane (20 ml), filtered through a Celite pad to remove elemental mercury and ethanol (10 ml) was then added. Removal of the dichloromethane on a rotary evaporator yielded bright orange–yellow crystals of **2a** (152 mg, 89%). M.p. 224–225°C. *m*/z 890.1075; $C_{43}H_{34}Cl_2OsOP_2$ requires 890.1077. Anal. Calc. for $C_{43}H_{34}Cl_2OsOP_2$: C, 58.04; H, 3.85. Found: C, 57.58; H, 3.82%.

3.5. *Os(C_6H_4Br-2)Cl(CO)(PPh_3)$_2$ (**2b**)*

To a dichloromethane solution (10 ml) of Os(C_6H_4Br-2)(η^2-O_2CCH_3)(CO)(PPh_3)$_2$ (**4**) (see Section 3.8) (50 mg, 0.052 mmol) one drop of HCl (conc.) in EtOH (5 ml) was added. The resulting bright yellow solution was reduced in volume on the rotary evaporator and yellow crystals of **2b** were filtered off and collected (47 mg, 97%). *m*/*z* 934.0581; $C_{43}H_{34}OBrClOsP_2$ requires 934.0572. Anal. Calc. for $C_{43}H_{34}BrClOsOP_2$: C, 55.28; H, 3.67. Found: C, 55.46; H, 3.74%.

3.6. $Os(C_6H_4I\text{-}2)Cl(CO)(PPh_3)_2$ (**2c**)

$OsHCl(CO)(PPh_3)_3$ (200 mg, 0.192 mmol) was treated with $Hg(C_6H_4I\text{-}2)_2$ (129 mg, 0.211 mmol) as described for **2a** to give, after isolation, bright yellow crystals of **2c** (143 mg, 76%). M.p. 230°C. Anal. Calc. for $C_{43}H_{34}ClIOOsP_2{\cdot}CH_2Cl_2$: C, 49.57; H, 3.40. Found: C, 49.13; H, 3.14%.

3.7. $Ru(C_6H_4Br\text{-}2)(\eta^2\text{-}O_2CCH_3)(CO)(PPh_3)_2$ (**3**)

$RuHCl(CO)(PPh_3)_3$ (200 mg, 0.210 mmol) and $Hg(C_6H_4Br\text{-}2)_2$ (108 mg, 0.211 mmol) were added to toluene (50 ml) and the solution was heated under reflux for 24 h, cooled, and the toluene removed in vacuo. Dichloromethane (25 ml) and NaOAc (34 mg, 0.42 mmol) in H_2O:EtOH 1:9 ml were added to the residue. Evaporation of the solvent gave pale yellow crystals of **3** (133 mg, 73%). Anal. Calc. for $C_{45}H_{37}BrO_3RuP_2{\cdot}0.25CH_2Cl_2$: C, 61.08; H, 4.25. Found: C, 60.86; H, 4.29%.

3.8. $Os(C_6H_4Br\text{-}2)(\eta^2\text{-}O_2CCH_3)(CO)(PPh_3)_2$ (**4**)

$OsHCl(CO)(PPh_3)_3$ (200 mg, 0.192 mmol) and $Hg(C_6H_4Br\text{-}2)_2$ (108 mg, 0.211 mmol) were treated as in Section 3.7 to give pale yellow crystals of **4** (136 mg, 74%). *m*/*z* 958.0935; $C_{45}H_{37}BrO_3OsP_2$ requires 958.1016. Anal. Calc. for $C_{45}H_{37}BrO_3OsP_2{\cdot}0.25C_7H_8$: C, 57.24; H, 4.01. Found: C, 57.27; H, 3.73%.

3.9. $Ru(C_6H_4Cl\text{-}2)Cl(CO)_2(PPh_3)_2$ (**5a**)

$Ru(C_6H_4Cl\text{-}2)Cl(CO)(PPh_3)_2$ (100 mg, 0.125 mmol) was dissolved in dichloromethane (25 ml) and the solution was added to a Fischer–Porter bottle. The bright yellow solution was subjected to carbon monoxide (4 atm) for 15 min, the pressure released, and ethanol (10 ml) was added. The solvent volume was reduced on a rotary evaporator to give colourless crystals of pure **5a** (94 mg, 91%). *m*/*z* 800, 793; $C_{43}H_{34}Cl_2OP_2Ru$ $[M^+ - CO]$ requires 800, $C_{44}H_{34}ClO_2P_2Ru$ $[M^+ - Cl]$ requires 793. Anal. Calc. for $C_{44}H_{34}Cl_2O_2P_2Ru{\cdot}0.25CH_2Cl_2$: C, 62.55; H, 4.09. Found: C, 62.65; H, 4.14%.

3.10. $Ru(C_6H_4Br\text{-}2)Cl(CO)_2(PPh_3)_2$ (**5b**)

$Ru(C_6H_4Br\text{-}2)(\eta^2\text{-}O_2CCH_3)(CO)(PPh_3)_2$ (100 mg, 0.118 mmol) was dissolved in dichloromethane (25 ml) and the solution added to a Fischer–Porter bottle. The solution was acidified with HCl (aq, one drop) and LiCl (20 mg, 0.472 mmol) was added. Subsequent treatment with carbon monoxide (4 atm), addition of ethanol (10 ml) and reduction of the solvent volume on a rotary evaporator yielded colourless crystals of **5b** that were filtered off and collected (89 mg, 86%). Anal. Calc. for $C_{44}H_{34}BrClO_2P_2Ru{\cdot}0.5CH_2Cl_2$: C, 58.40; H, 3.86. Found: C, 58.52; H, 3.88%.

3.11. $Os(C_6H_4Cl\text{-}2)Cl(CO)_2(PPh_3)_2$ (**6a**)

$Os(C_6H_4Cl\text{-}2)Cl(CO)(PPh_3)_2$ (100 mg, 0.112 mmol) was dissolved in dichloromethane (25 ml) and the solution was added to a Fischer–Porter bottle. The bright yellow solution was subjected to carbon monoxide (4 atm) for 15 min, the pressure released, and ethanol (10 ml) was added. The solvent volume was reduced on a rotary evaporator to give colourless crystals of pure **6a** that were filtered off and collected (90 mg, 87%). M.p. 220–221°C. *m*/*z* 890, 883; $C_{43}H_{34}Cl_2OOsP_2$ $[M^+ - CO]$ requires 890 $C_{44}H_{34}ClO_2OsP_2$ $[M^+ - Cl]$ requires 883. Anal. Calc. for $C_{44}H_{34}Cl_2O_2OsP_2$: C, 57.58; H, 3.73. Found: C, 57.27; H, 3.73%.

3.12. $Os(C_6H_4Br\text{-}2)Cl(CO)_2(PPh_3)_2$ (**6b**)

$Os(C_6H_4Br\text{-}2)(\eta^2\text{-}O_2CCH_3)(CO)(PPh_3)_2$ (100 mg, 0.107 mmol) was dissolved in dichloromethane (25 ml) and the solution added to a Fischer–Porter bottle. The solution was acidified with HCl (aq, one drop) and LiCl (20 mg, 0.472 mmol) was added. Subsequent treatment with carbon monoxide (4 atm), addition of ethanol (10 ml) and reduction of the solvent volume on a rotary evaporator yielded colourless crystals of **6b** that were filtered off and collected (90 mg, 87%). *m*/*z* 927.0832, $C_{44}H_{34}BrO_2OsP_2$ $[M^+ - Cl]$ requires 927.0832. Anal. Calc. for $C_{44}H_{34}BrClO_2OsP_2$: C, 54.92; H, 3.56. Found: C, 54.83; H, 3.58%.

3.13. $Os(C_6H_4I\text{-}2)Cl(CO)_2(PPh_3)_2$ (**6c**)

$Os(C_6H_4I\text{-}2)Cl(CO)(PPh_3)_2$ (100 mg, 0.102 mmol) was dissolved in dichloromethane (25 ml) and the solution added to a Fischer–Porter bottle and treated with carbon monoxide (4 atm), as described for **6a**, to yield colourless crystals of **6c** (89 mg, 89%). *m*/*z* 1010; $C_{44}H_{34}ClIO_2P_2Os$ requires 1010. Anal. Calc. for $C_{44}H_{34}ClIO_2P_2Os{\cdot}CH_2Cl_2$: C, 49.40; H, 3.32. Found: C, 49.37; H, 3.16%.

3.14. $Os(C_6H_4Cl\text{-}2)Cl(CS)(PPh_3)_2$ (**7a**)

$OsHCl(CS)(PPh_3)_3$ (200 mg, 0.189 mmol) was treated with $Hg(C_6H_4Cl\text{-}2)_2$ (90 mg, 0.21 mmol) as described for **2a**, except that the mixture was heated under reflux for 4 h, to give, after isolation, bright yellow crystals of complex **7a** (79%, 138 mg). *m*/*z* 906.0839; $C_{43}H_{34}Cl_2OsP_2S$ requires 906.0848. Anal. Calc. for $C_{43}H_{34}Cl_2OsP_2S$: C, 57.01; H, 3.78. Found: C, 56.51; H, 4.12%.

3.15. *$Os(C_6H_4Br\text{-}2)Cl(CS)(PPh_3)_2$* ***(7b)***

$OsHCl(CS)(PPh_3)_3$ (200 mg, 0.189 mmol) was treated with $Hg(C_6H_4Br\text{-}2)_2$ (107 mg, 0.208 mmol) as described for **2a** to give bright yellow crystals of **7b** (79%, 142 mg). *m*/*z* 950.0251; $C_{43}H_{37}ClBrOsP_2S$ requires 950.0343. Anal. Calc. for $C_{43}H_{37}ClBrOsP_2S$: C, 54.35; H, 3.61. Found: C, 54.05; H, 3.76%.

3.16. *$Os(C_6H_4Cl\text{-}2)Cl(CS)(CO)(PPh_3)_2$* ***(8a)***

$Os(C_6H_4Cl\text{-}2)Cl(CS)(PPh_3)_2$ (100 mg, 0.105 mmol) was dissolved in dichloromethane (25 ml) and the solution added to a Fischer–Porter bottle which was then pressured with carbon monoxide (4 atm). Ethanol (10 ml) was added, the dichloromethane removed on a rotary evaporator, and colourless crystals of **8a** were collected (78 mg, 76%). M.p. 224–225°C. *m*/*z* 906.0715, $C_{43}H_{34}Cl_2OsP_2S$ $[M^+ - CO]$ requires 906.0848; 899.1079, $C_{44}H_{34}ClOOsP_2S$ $[M^+ - Cl]$ requires 899.1109. Anal. Calc. for $C_{44}H_{34}Cl_2OOsP_2S{\cdot}H_2O$: C, 55.52; H, 3.81. Found: C, 55.77; H, 3.98%.

3.17. *$Os(C_6H_4Br\text{-}2)Cl(CS)(CO)(PPh_3)_2$* ***(8b)***

$Os(C_6H_4Br\text{-}2)Cl(CS)(PPh_3)_2$ (100 mg, 0.105 mmol) was dissolved in dichloromethane (25 ml) and the solution added to a Fischer–Porter bottle and treated with carbon monoxide to give a colourless solution. Ethanol (5 ml) was added, the dichloromethane (10 ml) removed on a rotary evaporator, and complex **8b** was filtered off and collected (78 mg, 76%). Anal. Calc. for $C_{44}H_{34}BrClOOsP_2S{\cdot}CH_2Cl_2$: C, 50.83; H, 3.41. Found: C, 50.42; H, 3.72%.

3.18. *$Os(\eta^2\text{-}CS\{C_6H_4Cl\text{-}2\})Cl(CO)(PPh_3)_2$* ***(9a)***

$Os(C_6H_4Cl\text{-}2)Cl(CO)(CS)(PPh_3)_2$ (100 mg, 0.105 mmol) was dissolved in toluene. After 5 min heating under reflux, the toluene was removed from the purplish–red solution in vacuo. The purple residue was redissolved in dichloromethane (15 ml), ethanol (5 ml) was added, and the dichloromethane removed on a rotary evaporator to give **9a** which was filtered off and subsequently recrystallised from dichloromethane: ethanol (15:5 ml) (88 mg, 88%). M.p. 225–226°C. *m*/*z* 934.0782, $C_{44}H_{34}Cl_2OOsP_2S$ requires 934.0798. Anal. Calc. for $C_{44}H_{34}Cl_2OOsP_2S{\cdot}CH_2Cl_2$: C, 53.05; H, 3.56. Found: C, 53.00; H, 3.66%.

3.19. *$Os(\eta^2\text{-}CS\{C_6H_4Br\text{-}2\})Cl(CO)(PPh_3)_2$* ***(9b)***

$Os(C_6H_4Br\text{-}2)Cl(CO)(CS)(PPh_3)_2$ (100 mg, 0.105 mmol) was dissolved in toluene (25 ml). After 5 min heating under reflux, the toluene was removed from the purplish–red solution and the residue was redissolved in dichloromethane (10 ml). Ethanol (5 ml) was added, and the dichloromethane was removed on a rotary evaporator to give purple crystals of complex **9b** which were further recrystallised from dichloromethane: ethanol (15:5 ml) (89 mg, 89%). *m*/*z* 978.0270; $C_{44}H_{34}BrClOOsP_2S$ requires 978.0292. Anal. Calc. for $C_{44}H_{34}BrClOOsP_2S{\cdot}CH_2Cl_2$: C, 50.83; H, 3.41. Found: C, 50.62; H, 3.83%.

3.20. *$Os(\eta^2\text{-}CS\{C_6H_4SnBu_3\text{-}2\})Cl(CO)(PPh_3)_2$* ***(10)***

$Os(\eta^2\text{-}CS\{C_6H_4Br\text{-}2\})Cl(CO)(PPh_3)_2$ (100 mg, 0.102 mmol) was dissolved in dry, deoxygenated THF (50 ml) at 40°C. The deep-purple solution was cooled to − 78°C and a solution of ^{n}BuLi (0.102 ml, 1 M, 0.102 mmol) was added. The colour changed instantly to bright orange. The solution was stirred for 5 min at − 78°C and Bu_3SnCl (0.139 ml, 0.425 mmol) was added slowly. The solution was allowed to warm to r.t., during which time it reverted from bright orange to a dark purple colour. Water and ethanol were added and the THF was removed on a rotary evaporator. The red solid was decanted from the solution, filtered off, and recrystallised from dichloromethane:hexane (20:5 ml) to yield purplish–red crystals of **10** (81 mg, 67%). Anal. Calc. for $C_{56}H_{61}ClOOsP_2SSn$: C, 56.60; H, 5.17. Found: C, 56.70; H, 5.32%.

3.21. *X-ray crystal structure determinations of* ***2a***, ***2b***, ***2c***, ***6a***, ***8a***, ***9a*** *and* ***9b***

X-ray data collection for **2a**, **2b**, **2c**, **6a**, **8a**, **9a** and **9b** was on a Siemens SMART diffractometer with a CCD area detector, using graphite monochromated Mo–K_α radiation ($\lambda = 0.71073$ Å). Data were integrated and Lorentz and polarisation correction applied using SAINT [16] software. Semi-empirical absorption corrections were applied based on equivalent reflections using SADABS [17]. The structures were solved by Patterson and Fourier methods and refined by full-matrix least-squares on F^2 using programs SHELXS [18] and SHELXL [19]. Complexes **2a**, **2b** and **2c** are isostructural as are **9a** and **9b**. In these cases the known structure was used as a starting point for the subsequent refinements. All non-hydrogen atoms were refined anisotropically and hydrogen atoms were included in calculated positions and refined with a riding model with thermal parameter 20% greater than U_{iso} of the carrier atom. Crystal data and refinement details are given in Table 4.

4. Supplementary material

Crystallographic data (excluding structure factors) for the structures reported have been deposited with the

Cambridge Crystallographic Data Centre as supplementary publication nos. 139392–139398 for **2a**, **2b**, **2c**, **6a**, **8a**, **9a** and **9b**, respectively. Copies of this information can be obtained free of charge from the Director, CCDC, 12 Union Road, Cambridge, CB2 1EZ, UK (fax: +44-1223-336033; e-mail: deposit@ccdc.cam.ac.uk or www: http://www.ccdc.cam.ac.uk.

Acknowledgements

We thank the University of Auckland Research Committee for partial support of this work through grants-in-aid and through the award of a Doctoral Scholarship to SDW.

References

[1] (a) S.B. Miller, B.L. Jelus, J.H. Smith, B. Munson, T.B. Brill, J. Organomet. Chem. 170 (1979) 9. (b) N.A.A. Al-Jabar, A.G. Massey, J. Organomet. Chem. 288 (1985) 145. (c) K. Mochida, T. Yamanishi, J. Organomet. Chem. 322 (1987) 247. (d) C. Eaborn, B. Singh, J. Organomet. Chem. 177 (1979) 333. (e) M. Schürmann, F. Huber, J. Organomet. Chem. 530 (1997) 121. (f) F. Huber, H. Preut, D. Scholz, M. Schürmann, J. Organomet. Chem. 441 (1992) 227.

[2] (a) D.R. Fahey, J. Am. Chem. Soc. 92 (1970) 402. (b) D.R. Fahey, J.E. Mahan, J. Am. Chem. Soc. 99 (1977) 2501. (c) C. Butler, C. Eaborn, A. Pidcock, J. Organomet. Chem. 144 (1978) C23. (d) M. Crespo, J. Sales, X. Solans, M.F. Altaba, J. Chem. Soc. Dalton Trans. (1988) 1617. (e) M. Crespo, J. Sales, J. Organomet. Chem. 322 (1987) 405. (f) M. Crespo, O. Rosell, J. Sales, M. Reco, J. Organomet. Chem. 273 (1984) 415.

[3] (a) M.A. Bennett, T.W. Hambley, N.K. Roberts, G.B. Robertson, Organometallics 4 (1985) 1992. (b) M.A. Bennett, E. Wenger, Chem. Ber. 130 (1997) 1029. (c) M.A. Bennett, D.C.R. Hockless, E. Wenger, Polyhedron 14 (1995) 2637. (d) M.A. Bennett, T. Dirnberger, D.C.R. Hockless, E. Wenger, A.C. Willis, J. Chem. Soc. Dalton Trans. (1998) 271.

[4] (a) W.R. Roper, L.J. Wright, J. Organomet. Chem. 142 (1977) C1. (b) C.E.F. Rickard, W.R. Roper, G.E. Taylor, J.M. Waters, L.J. Wright, J. Organomet. Chem. 389 (1990) 375. (c) M.M.P. Ng, W.R. Roper, L.J. Wright, Organometallics 13 (1994) 2563. (d) G.R. Clark, M.M.P. Ng, W.R. Roper, L.J. Wright, J. Organomet. Chem. 491 (1995) 219. (e) K. Hübler, U. Hübler, W.R. Roper, L.J. Wright, J. Organomet. Chem. 526 (1996) 199. (f) A.M. Clark, C.E.F. Rickard, W.R. Roper, L.J. Wright, J. Organomet. Chem. 545–546 (1997) 619.

[5] G.R. Clark, C.E.L. Headford, W.R. Roper, L.J. Wright, V.P.D. Yap, Inorg. Chim. Acta 220 (1994) 261.

[6] L.G. Makarova, A.N. Nesmeyanov, The Organic Compounds of Mercury, North-Holland, Amsterdam, 1967.

[7] R.H. Crabtree, J.W. Faller, M.F. Mellea, J.M. Quirk, Organometallics 1 (1982) 1361.

[8] M.D. Butts, B.L. Scott, G.L. Kubas, J. Am. Chem. Soc. 118 (1996) 11831.

[9] G.R. Clark, T.J. Collins, K. Marsden, W.R. Roper, J. Organomet. Chem. 259 (1983) 215.

[10] S.M. Maddock, C.E.F. Rickard, W.R. Roper, L.J. Wright, Organometallics 15 (1996) 1793.

[11] P.S. Hallman, B.R. McGarvey, G. Wilkinson, J. Chem. Soc. (A) (1968) 3143.

[12] L. Vaska, J. Am. Chem. Soc. 86 (1964) 1943.

[13] G.P. Elliott, N.M. McAuley, W.R. Roper, Inorg. Synth. 26 (1989) 184.

[14] (a) M.E. Hanke, J. Am. Chem. Soc. 45 (1923) 1321. (b) M.S. Kharasch, H. Pines, J.H. Levine, J. Org. Chem. 3 (1938) 347.

[15] (a) L.M. Yagupol'skii, V.I. Popov, N.V. Kondratenko, Zh. Org. Khim. 12 (1976) 916. (b) R.P. Rao, S.H. Singh, S. Raj, N.B. Zaidi, B. Singh, Indian J. Chem. Sect. B 18 (1979) 377.

[16] SAINT, Area detector integration software, Siemens Analytical Instruments Inc., Madison, WI, 1995.

[17] G.M. Sheldrick, SADABS, Program for semi-empirical absorption correction, University of Göttingen, Germany, 1977.

[18] G.M. Sheldrick, SHELXS, Program for crystal structure determination, University of Göttingen, Germany, 1977.

[19] G.M. Sheldrick, SADABS, Program for crystal structure refinement, University of Göttingen, Germany, 1977.